



OPEN ACCESS

EDITED BY
Qitong Huang,
Gannan Medical University, China

REVIEWED BY
Zhijin Fan,
Sun Yat-sen University, China
Hani Nasser Abdelhamid,
Assiut University, Egypt

*CORRESPONDENCE
Xiaojun Liu,
drluixiaojun@163.com
Hao Tang,
tangpku_zzuhao@zzu.edu.cn
Qian Bai,
baiqian@zzu.edu.cn

[†]These authors have contributed equally to this work

SPECIALTY SECTION
This article was submitted to
Nanobiotechnology,
a section of the journal
Frontiers in Bioengineering and
Biotechnology

RECEIVED 12 July 2022
ACCEPTED 03 August 2022
PUBLISHED 31 August 2022

CITATION
Li Q, Feng R, Chang Z, Liu X, Tang H and
Bai Q (2022), Hybrid biomimetic
assembly enzymes based on ZIF-8 as
“intracellular scavenger” mitigating
neuronal damage caused by
oxidative stress.
Front. Bioeng. Biotechnol. 10:991949.
doi: 10.3389/fbioe.2022.991949

COPYRIGHT
© 2022 Li, Feng, Chang, Liu, Tang and
Bai. This is an open-access article
distributed under the terms of the
[Creative Commons Attribution License
\(CC BY\)](https://creativecommons.org/licenses/by/4.0/). The use, distribution or
reproduction in other forums is
permitted, provided the original
author(s) and the copyright owner(s) are
credited and that the original
publication in this journal is cited, in
accordance with accepted academic
practice. No use, distribution or
reproduction is permitted which does
not comply with these terms.

Hybrid biomimetic assembly enzymes based on ZIF-8 as “intracellular scavenger” mitigating neuronal damage caused by oxidative stress

Qing Li^{1†}, Ruixia Feng^{2†}, Zhaohui Chang^{1†}, Xiaojun Liu^{2*},
Hao Tang^{3*} and Qian Bai^{2*}

¹Department of Molecular Pathology, Application Center for Precision Medicine, The Second Affiliated Hospital of Zhengzhou University, Zhengzhou, China, ²Department of Critical Care Medicine, Second Affiliated Hospital of Zhengzhou University, Zhengzhou, China, ³National Health Commission Key Laboratory of Cardiovascular Regenerative Medicine, Heart Center of Henan Provincial People's Hospital, Central China Fuwai Hospital of Zhengzhou University, Fuwai Central China Cardiovascular Hospital and Central China Branch of National Center for Cardiovascular Diseases, Zhengzhou, China

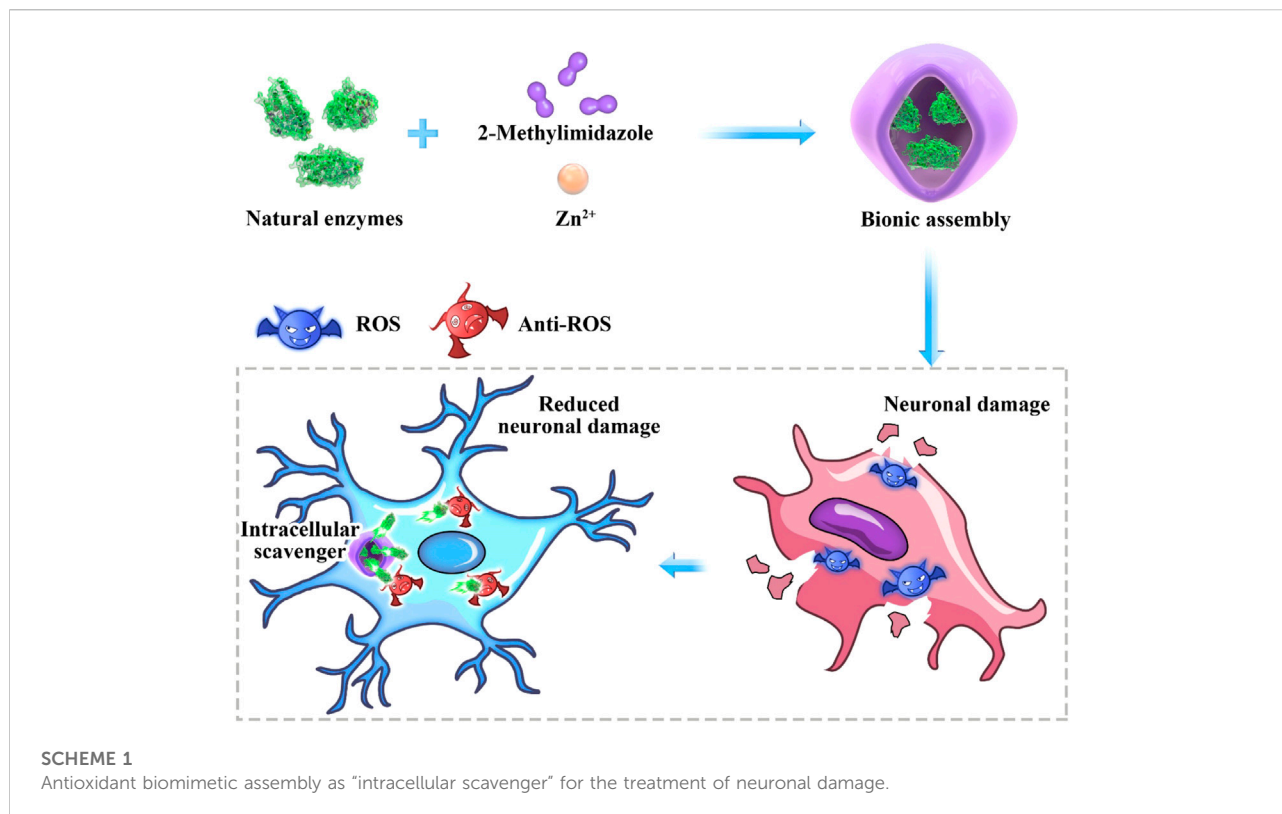
Superoxide dismutase (SOD) was immobilized in zeolite imidazolate framework-8 (ZIF-8) through biomimetic mineralization method, namely SOD@ZIF-8, which was then used in the treatment of nerve damage by eliminating reactive oxygen species (ROS). A series of chemical characterization and enzymatic activity researches revealed that SOD was successfully embedded into ZIF-8 without apparent influence on the antioxidant activity of SOD. Cell level experiments showed that SOD@ZIF-8 could be effectively endocytosed by cells. The activity of SOD@ZIF-8 in scavenging ROS played a critical role in protecting SHSY-5Y cells from MPP⁺-induced cell model and relieving cell apoptosis, indicating that SOD@ZIF-8 could effectively rescue ROS-mediated neurological disorders though removing excessive ROS produced *in vitro*.

KEYWORDS

biomimetic mineralization, SOD@ZIF-8, nerve damage, ROS scavenging, neurological disorders

Introduction

Reactive oxygen species (ROS), which is frequently mentioned in the field of biology and medicine, refers to oxygen-containing substances with high reactivity, specific including superoxide anion (O₂⁻), hydrogen peroxide (H₂O₂), hydroxyl radical (OH), singlet oxygen (¹O₂), peroxide free radical (LOO), hydrogen peroxide lipid (LOOH), peroxy group (ONOO⁻), hypochlorous acid (HOCl), ozone (O₃) and so on. ROS generated in the process of oxygen metabolism are essential for cell signaling and immune response (Finkel, 2011; Sena and Chandel, 2012). However, the excessive expression of ROS is deleterious especially in the brain, since it induces oxidative damage of protein,



lipid and DNA. As such, ROS are highly responsible for the development of many nerve damage such as cerebral palsy, Alzheimer's diseases, schizophrenia and Parkinson's diseases (PD) (Dietrich-Muszalska and Kontek, 2010; Popa-Wagner et al., 2013; Yan et al., 2013). Superoxide dismutase (SOD), as a crucial member of the antioxidant system, can efficiently catalyze the decomposition of superoxide radical to hydrogen peroxide and oxygen (Hall et al., 2010; Hu and Tirelli, 2012; Van Raamsdonk and Hekimi, 2012). Therefore, it has demonstrated therapeutic potential in the treatment of ROS-mediated diseases including inflammation, diabetes, radiation injuries, and central nervous system (CNS) disorders (Seshadri et al., 2010; Wang et al., 2010). However, due to the relatively instability character and short intracellular half-lives of proteins, direct use of SOD has been hampered by poor pharmacokinetics, rapid renal clearance, degradation by proteases in the serum and low cellular membranes penetrating ability (Tong et al., 2012; Chen et al., 2013; Liu et al., 2021a; Li et al., 2022a). Thus, to enhance SOD stability and bioavailability with desirable catalytic activity, immobilization method has been investigated by using different solid supports such as organic polymers, magnetic nanoparticles and mesoporous silica (Wu and Yang, 2017; Li et al., 2021). Among these materials, metal-organic frameworks (MOFs), consisting by metal ions nodes and organic ligands, have been increasingly proven to be a robust solid support in the

enzyme immobilization due to its large surface area, tunable porosity and functionality, favorable excellent thermal/mechanical stability (Orellana-Tavra et al., 2015; Lian et al., 2016; Lian et al., 2017; Abdelhamid, 2021; Hoseinpour and Shariatinia, 2021; Li et al., 2022b). Generally, MOF-based immobilization approaches are mainly included by physical adsorption or entrapment, which have demonstrated unique advantages such as high loading efficiency of enzymes and excellent stability against high temperature and organic solvents (Ding et al., 2021). Nevertheless, these strategies are not able to achieve the size control of enzyme-MOF composites and maintain the enzymatic activity due to MOF-induced destabilization of enzymes' conformation. Recently, biomimetic mineralization approach for MOF synthesis has been adopted to encapsulate the enzyme molecules within protective exteriors through self-assembly process (Liang et al., 2015; Chen and Ma, 2016; Liang et al., 2016; Mehta et al., 2016; Abdelhamid, 2020; Fan et al., 2021). These enzyme-MOF composites are able to solve the unfavorable solvent effect of enzymatic structure and limited loading of large enzyme into MOF pores. Unlike other encapsulation approaches such as coprecipitation, enzyme molecules can trigger nucleation of porous crystals by concentrating the MOF building blocks in the process of biomimetic mineralization (Xie et al., 2010; He et al., 2016; Jiang et al., 2017; Zhu et al., 2022). Notably, enzyme-

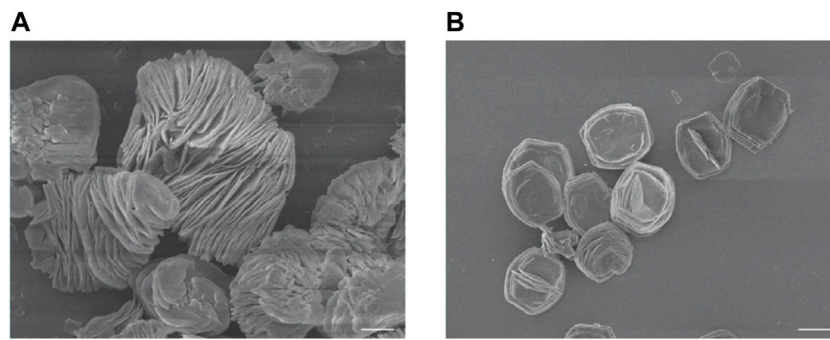


FIGURE 1
SEM images of ZIF-8 with the molar ratios of 2-dimethylimidazole and zinc acetate at 4:1 (A) and 24:1 (B). The scale bars are 5 µm.

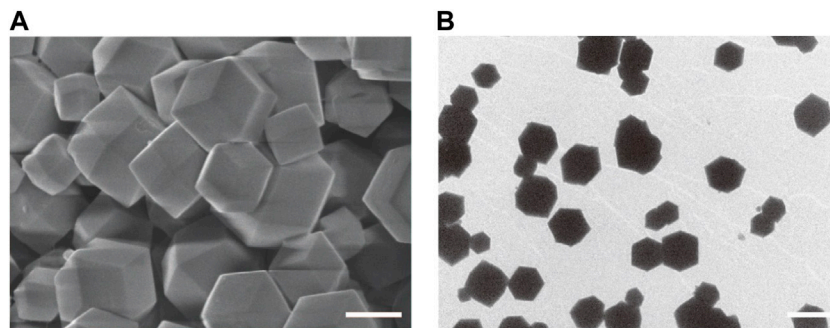


FIGURE 2
SEM images (A) and TEM images (B) of SOD@ZIF-8. The scale bars are 100 nm for A and 200 nm for (B)

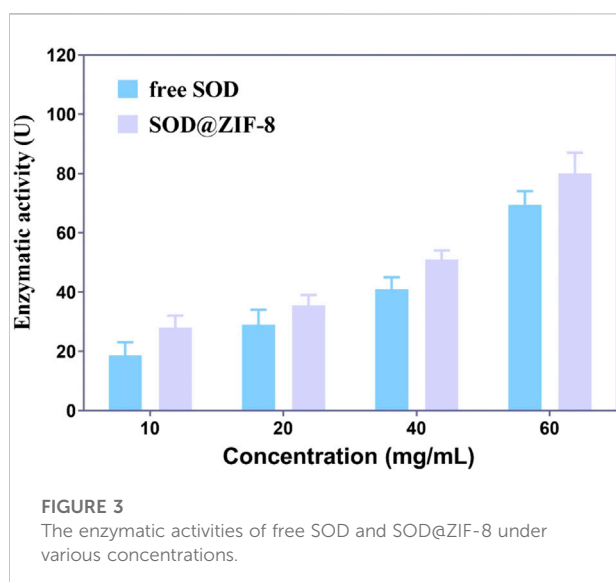


FIGURE 3
The enzymatic activities of free SOD and SOD@ZIF-8 under various concentrations.

MOF composites obtained from this method can enlarge the bioactive temperature range of enzyme and enhance the stability in a facile manner, demonstrating a great promise in the biomedical application (Montanari et al., 2012; Tabrez et al., 2012; Zhu et al., 2012; Li et al., 2020; Yang et al., 2020).

Herein, SOD was embedded into zeolite imidazolate framework-8 (ZIF-8) through biomimetic mineralization method (denoted as SOD@ZIF-8). The SOD@ZIF-8 assembly was then employed as ROS scavenger in neuronal damage treatment. Significantly, a neuronal damage cell model was established to evaluate the therapeutic effect of SOD@ZIF-8 (Scheme 1).

Results and discussion

Firstly, ZIF-8 with various molar ratios of 2-dimethylimidazole/ Zn^{2+} (4:1, 24:1 and 48:1) were synthesized

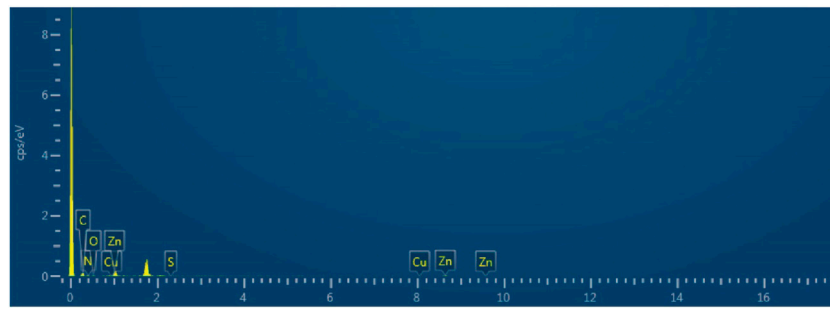


FIGURE 4
Elemental analysis of SOD@ZIF-8.

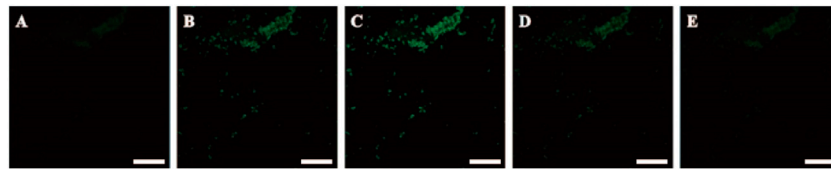


FIGURE 5
CLSM photographs of FITC-SOD@ZIF-8 with various depth at the z-axis of (A) 50 nm, (B) 100 nm, (C) 150 nm, (D) 200 nm, (E) 250 nm. 488 and 530 nm were chosen as the wavelengths for the detection of the fluorescence of FITC. The scale bars are 200 μ m.

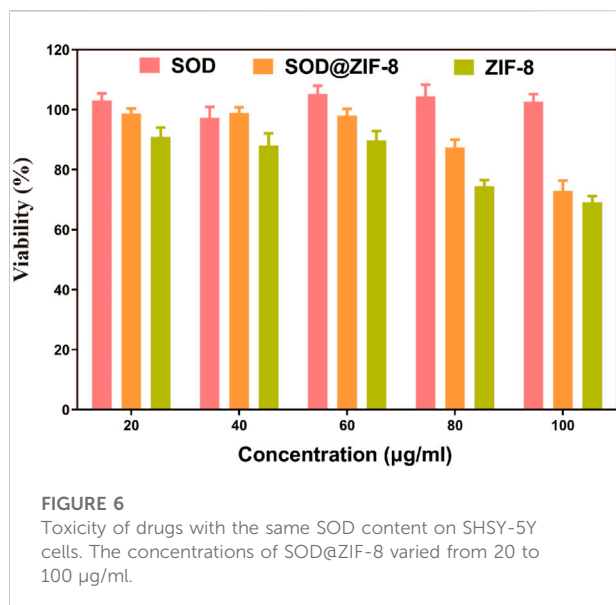


FIGURE 6
Toxicity of drugs with the same SOD content on SHSY-5Y cells. The concentrations of SOD@ZIF-8 varied from 20 to 100 μ g/ml.

to investigate the suitable morphology and particle size for biomedical applications. As shown in Figure 1, micro-scaled SOD@ZIF-8 composites with size of more than 3 μ m were obtained at the molar ratios of 4:1 and 24:1, respectively.

Moreover, their morphology is too irregular to illustrate a single assembly enzyme complex. When the molar ratio was fixed at 48:1, regular dodecahedron structure and smaller size of SOD@ZIF-8 with 150–200 nm was achieved, which was preferable for the biomedical applications. Further, SOD was immobilized into ZIF-8 through biomimetic mineralization method. SEM and TEM images (Figure 2) suggested that the morphology and particle size did not change significantly compared with me-ZIF-8. Importantly, after ZIF-8 immobilization, the SOD activity was improved compared with free SOD (Figure 3), suggesting the biomimetic mineralization strategies could help enhance the enzymatic activities of SOD. This phenomenon might result from the fact that ZIF-8 benefit the dispersion of SOD, thus exposing more enzyme-activity centers and promoting enzymatic activity.

Meanwhile, chemical elements analysis of SOD@ZIF-8 showed the presence of Cu signal in the composites, presenting immobilization of enzyme harboring Cu element in ZIF-8 through biomimetic mineralization (Figure 4). To further validate the efficient assembly of SOD enzyme, SOD was labeled with fluorescein isothiocyanate (FITC) and then incorporated into ZIF-8 to construct FITC-labeled SOD@ZIF-8 through biomimetic mineralization. As shown in (Figure 5), green fluorescence of FITC-labeled SOD was clearly shown in the SOD@ZIF-8 assembling enzyme through laser confocal

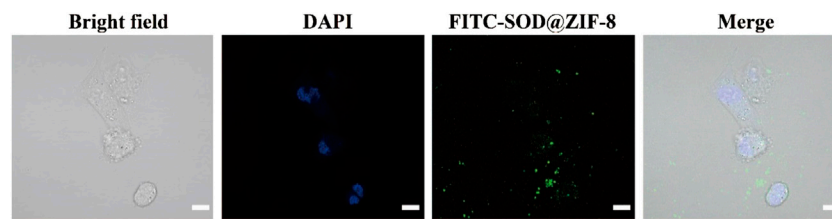


FIGURE 7
Cellular uptake ability of SOD@ZIF-8 detected by CLSM.

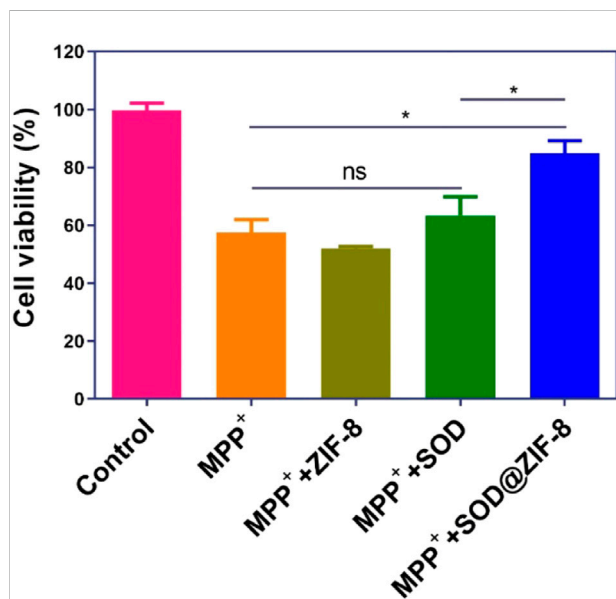


FIGURE 8
Viability of SHSY-5Y cells exposed to MPP⁺ after different treatments.

microscope. The fluorescence intensity of FITC showed a gradually increasing trend from the peak to the middle and then reduced to the bottom, indicating the successful incorporation of SOD into ZIF-8. Besides, The BCA result suggested that the loading efficiency of SOD in SOD@ZIF-8 was 23.43 wt%, which was a relatively high level among the reports of SOD immobilization.

To investigate the applications of SOD@ZIF-8 composites *in vitro*, cell viability was examined to determine their potential cytotoxicity through MTT assay. As shown in Figure 6, compared with pure ZIF-8, the entrapment of SOD into ZIF-8 through biomimetic mineralization significantly reduced the cytotoxicity of ZIF-8 at various concentrations of 20–100 µg/ml. Negligible cytotoxicity was observed in SOD@ZIF-8 composites at the concentration of 60 µg/ml, indicating that SOD@ZIF-8 presented a satisfactory biocompatibility against cells. Subsequently, SOD was labeled with FITC and then employed to determine the cellular uptake of SOD@ZIF-8 by fluorescence microscope. As shown in Figure 7, strong green fluorescence was observed in FITC-SOD@ZIF-8 nanocomposites-treated cells, and It can be clearly found that the particles are located in the cell rather than on the cell surface, verifying that SOD@

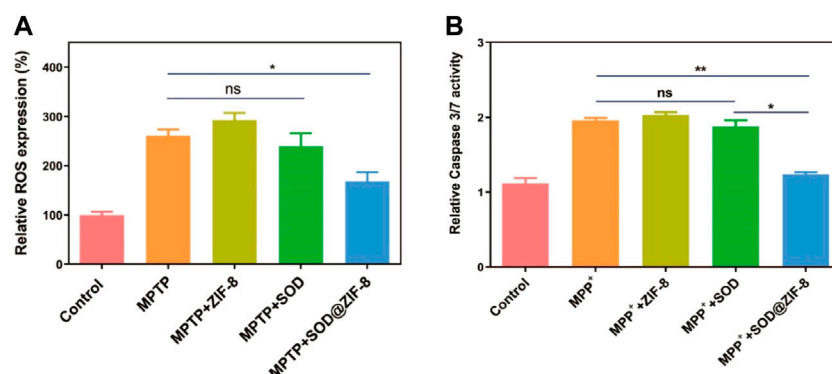


FIGURE 9
ROS scavenging activity of various nanomaterials in MPP⁺ treated SHSY-5Y cells detected by flow cytometry with DCFDA-H2 dye (A) and the detection of apoptosis by measuring the activity of effector caspase-3/7 (B).

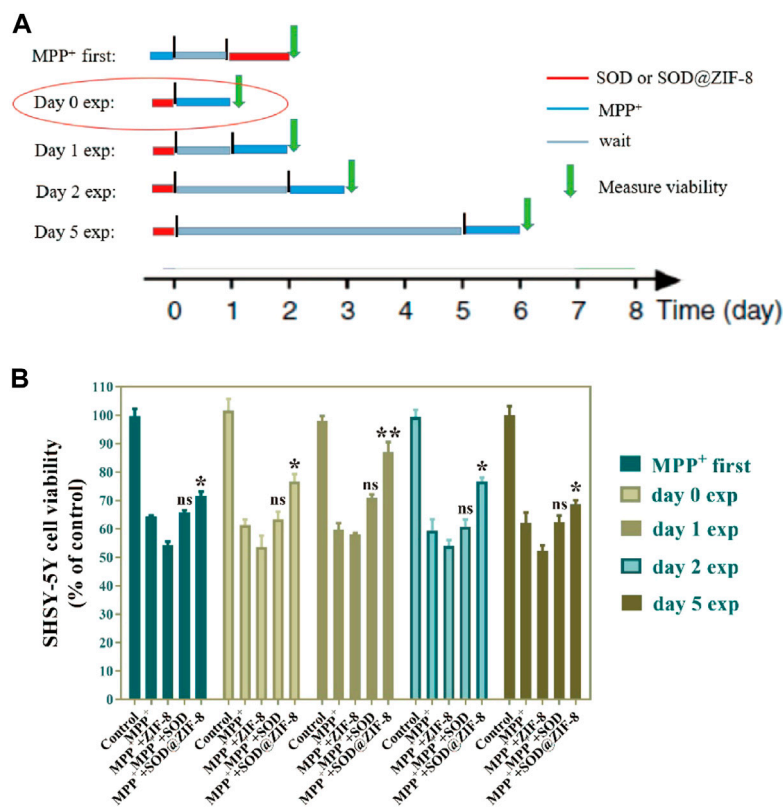


FIGURE 10

Long-term persistence effect of SOD@ZIF-8. Cells were pretreated with MPP⁺ (MPP⁺ first) or pretreated with SOD@ZIF-8 (Day 0 exp to Day 5 exp), washed and continued to culture for several days (gray time period in schematic diagram) and then exposed to MPP⁺ for 24 h. Cell viability was quantified by MTT assay.

TABLE 1 Study on the diagnosis and treatment of oxidation-related diseases based on ZIF-8 nanomaterials.

Nanomaterials	Particle sizes	Antioxidants	Antioxidant activity	Treatment of disease	References
CeO ₂ @ZIF-8	About 100 nm	CeO ₂	SOD, CAT	ischemic stroke	He et al. (2020)
SOD@ZIF-8	About 150 nm	SOD	SOD	Noise-induced hearing loss	Zhang et al. (2022)
ZIF-8@PB-QCT	About 100 nm	PB-QCT	SOD, CAT	Parkinson's disease	Liu et al. (2021b)

ZIF-8 were efficiently uptake by cells. The superior endocytosis of SOD@ZIF-8 composites by cells was mainly attributed to the nanosized structure, which was essential for intracellular release of SOD to cleave ROS *in vitro*.

For these encouraging advantages, we then investigated the ROS scavenging ability of SOD@ZIF-8 composites. 1-Methyl-4-phenylpyridinium (MPP⁺) as a neurotoxin was able to cause cell death in human neuroblastoma SH-SY5Y cells due to the intracellular elevation of ROS and apoptosis induction, which typically was used to resemble nerve damage

phenotype (Ding et al., 2021). As shown in Figure 8, obvious cell death was exhibited after SH-SY5Y cells were incubated with 2 mM MPP⁺. In contrast, cells pre-treated with SOD@ZIF-8 composites demonstrated an increasing viability after exposure to MPP⁺, confirming the protection afforded by SOD@ZIF-8 composites against neurotoxin. Subsequently, 2',7'-dichlorodihydrofluorescein diacetate (DCFH-DA), which was used to directly measure the redox state of cells, were adopted to detect ROS generation of SH-SY5Y cells. As shown in Figure 9A, SH-SY5Y cells treated with MPP⁺

exhibited an enhanced expression of ROS, leading to the cell death. Meanwhile, a significant decrease of ROS expression was achieved after SOD@ZIF-8 composites treatment, which was in agreement with MTT results. To confirm the protective effect of SOD@ZIF-8 composites, the activity of caspase-3 was detected. As illustrated in [Figure 9B](#), compared with untreated cells, MPP⁺ treatment triggered caspase-3 activation, leading to the apoptotic death of SH-SY5Y cells. However, a significant decrease of caspase-3 expression was achieved in SOD@ZIF-8 treatment, revealing that SOD@ZIF-8 composites inhibited apoptotic effect by downregulation of caspase-3.

To assess the long-term therapeutic effect of SOD@ZIF-8 composites, SH-SY5Y cells were incubated with SOD@ZIF-8 in advance, subsequently treated with MPP⁺ following several days. As shown in [Figure 10](#), SOD@ZIF-8 composites achieved a better protective effect compared with free SOD during 1, 2 and 5 days. Meanwhile, the protective effect afforded by SOD@ZIF-8 composites was gradually decreased in a time-dependent manner, where still 70% cell viability was achieved after 5-days treatment. These results could confirm that biomimetically mineralized enzymes maintained a persistent protective effect for cells. Interestingly, simultaneous administration of SOD@ZIF-8 composites and MPP⁺ demonstrated a little lower protective effect, which was probably caused by the delayed release of SOD from SOD@ZIF-8 composites after cellular uptake. Similarly, less protective effect was achieved when cells were pre-incubated with MPP⁺ and then treated with SOD@ZIF-8, indicating that SOD@ZIF-8 composites was attributed to prevention of MPP⁺-induced cell damage. These results demonstrated that biomimetically mineralized SOD@ZIF-8 provided a strong therapeutic efficacy and possessed a persistent protective effect in SH-SY5Y cells. In comparison with other reports concerning about treatment of oxidative damage diseases based on ZIF-8 nanomaterials, our study exhibits satisfactory antioxidant duration and therapeutic effects ([Table 1](#)) ([He, 2020](#); [Zhang, 2022](#); [Liu, 2021b](#)). We believe that this study has important implications for the application of ZIF-8-based antioxidant nanomaterials in neurodegenerative diseases, as well as other diseases associated with oxidative damage.

Conclusion

In summary, SOD was successfully immobilized in the ZIF-8 through biomimetic mineralization method. The composite SOD@ZIF-8 showed satisfactory enzymatic activity and excellent stability against temperature, pH and ion environment. Moreover, compared with free SOD, SOD@ZIF-8 composites were capable of realizing efficient cellular uptake to scavenge intracellular ROS induced by MPP⁺ in

neuroblasts, benefiting the cell survival state and cell activity significantly. Our study suggested that SOD@ZIF-8 composites could be employed as a potential approach for the treatment of nerve damage and other oxidative stress-stimulated neurological disorders.

Methods

Construction of SOD@ZIF-8 through biomimetic mineralization

The SOD@ZIF-8 composites through biomimetic mineralization was constructed according to previous reports ([Fan et al., 2021](#); [Zhu et al., 2022](#)). Briefly, 2 ml of 2-methylimidazole (HMeIM) solution (15.68 mg/ml) was mixed with 2 ml of Zn(OAc)₂ solution (8.76 mg/ml), 200 μ L of methanol and 1 ml of SOD solution (1 mg/ml). The compound was incubated at room temperature for 24 h, and then solids were collected by centrifugation and washed until no absorbance at 280 nm could be detected in the supernatant. Subsequently, solids were lyophilized to obtain SOD@ZIF-8 composites. The SOD loading in ZIF-8 was determined by BCA assay kit (Beyotime, Nanjing, China). Synthesis of FITC-SOD@ZIF-8.

20 mg SOD and 10 mg FITC were dissolved in 50 ml of PBS (50 mM, pH 8.0) and the mixture was stirred at room temperature for 24 h in the dark. The mixture was dialyzed against distilled water using Amicon[®] Ultra-15 ultrafiltration tube (Millipore, MA) until no absorbance at 488 nm could be detected in the supernatant and then lyophilized to obtain FITC-SOD. Compound FITC-SOD@ZIF-8 was constructed as described in the above section.

SOD enzymatic activity detection

SOD enzymatic activity was determined by nitro blue tetrazolium (NBT) assay and pyrogallol autoxidation assay. For NBT assay, solution containing 75 μ M NBT, 13 mM methionine, 20 μ M riboflavin, and free SOD or SOD@ZIF-8 were mixed in PBS buffer (25 mM, pH 7.4), respectively. The mixtures were detected at the absorbance at 560 nm using UV-2700 spectrophotometer (Shimadzu, Kyoto, Japan). For pyrogallol autoxidation assay, 240 μ L enzyme solutions (1 mg/ml) was added to 750 μ L Tris-HCL (pH 8.2) and incubated for 20 min 10 μ L pyrogallol solution (50 mM) was then mixed into the enzyme solutions and the absorbance at 325 nm was measured for 1 min by UV-2700 spectrometer (Shimadzu, Kyoto, Japan). Characterization of SOD@ZIF-8 Composites.

After depositing samples evenly onto a rigorously cleaved silicon wafer surface, scanning electron microscopy (SEM)

images and elemental analysis of SOD@ZIF-8 were obtained on a Hitachi FE-SEM S-4800 instrument with an acceleration voltage of 3 kV. Transmission electron microscopy (TEM) was carried on a JEM-2100F field emission electron microscope with an acceleration voltage of 200 kV.

Cell viability assay

SH-SY5Y cells were seeded into 96-well plates at a density of 7,000 cells/well overnight. Different formulations were added into the cells for 6 h and 2 mM MPP⁺ was subsequently added for 24 h. 20 μ L of MTT solution (5 mg/ml) was added into each well and incubated at 37°C for another 4 h. Finally, dimethyl sulfoxide (DMSO) was used to dissolve the formed formazan crystal and the absorbance at 492 nm was measured by a GF-M3000 microplate reader (CAIHONG, Shandong, China).

ROS detection of SH-SY5Y cells

ROS levels in SHSY-5Y cells were determined according to Reactive Oxygen Species Assay Kit (Beyotime, Nanjing, China). SH-SY5Y cells were seeded into 6-well plates at a density of 2.0×10^5 cells per well and pre-treated with different formulations for 6 h. Cells were then exposed to 2 mM MPP⁺ for 2 h at 37°C and stained with 10 μ M DCFH-DA for 20 min at 37°C. ROS expression was detected by flow cytometry (Accuri C6, Beckman, NJ) and analyzed using Beckman Coulter software.

Statistical analysis

GraphPad Prism 8.0.2 was utilized for all statistical analyses. The outcomes were compared via Student's *t*-tests. **p* < 0.01, ***p* < 0.005, ****p* < 0.001.

References

- Abdelhamid, H. N. (2020) Biointerface between ZIF-8 and biomolecules and their applications. *Biointerface Res. Appl. Chem.* 11 (1), 8283–8297.
- Abdelhamid, H. N. (2021). Zeolitic imidazolate frameworks (ZIF-8) for biomedical applications: A review. *Curr. Med. Chem.* 28 (34), 7023–7075. doi:10.2174/0929867328666210608143703
- Chen, Y.-P., Chen, C.-T., Hung, Y., Chou, C.-M., Liu, T.-P., Liang, M.-R., et al. (2013). A new strategy for intracellular delivery of enzyme using mesoporous silica nanoparticles: Superoxide dismutase. *J. Am. Chem. Soc.* 135 (4), 1516–1523. doi:10.1021/ja3105208
- Chen, Y., and Ma, S. (2016). Biomimetic catalysis of metal–organic frameworks. *Dalton Trans.* 45 (24), 9744–9753. doi:10.1039/c6dt00325g
- Dietrich-Muszalska, A., and Kontek, B. (2010). Lipid peroxidation in patients with schizophrenia. *Psychiatry Clin. Neurosci.* 64 (5), 469–475. doi:10.1111/j.1440-1819.2010.02132.x
- Ding, S., Liu, Z., Huang, C., Zeng, N., Jiang, W., and Li, Q. (2021). Novel engineered bacterium/black phosphorus quantum dot hybrid system for hypoxic

Data availability statement

The original contributions presented in the study are included in the article/supplementary material, further inquiries can be directed to the corresponding authors.

Author contributions

QL, RF, ZC: Complete research and manuscript writing, XL, HT, QB: Propose design concepts and review manuscripts.

Funding

The authors are grateful for the financial support from the Henan Medical Science and Technology Research Youth Project Co-Sponsored by the Province and Ministry in China (No: SBGJ202103088). Young and middle-aged academic leaders of health in Henan Province (No: HNSWJW-2021001).

Conflict of interest

The authors declare that the research was conducted in the absence of any commercial or financial relationships that could be construed as a potential conflict of interest.

Publisher's note

All claims expressed in this article are solely those of the authors and do not necessarily represent those of their affiliated organizations, or those of the publisher, the editors and the reviewers. Any product that may be evaluated in this article, or claim that may be made by its manufacturer, is not guaranteed or endorsed by the publisher.

tumor targeting and efficient photodynamic therapy. *ACS Appl. Mat. Interfaces* 13, 10564–10573. doi:10.1021/acsami.0c20254

Fan, Z., Liu, H., Xue, Y., Lin, J., Fu, Y., Xia, Z., et al. (2021). Reversing cold tumors to hot: An immunoadjuvant-functionalized metal-organic framework for multimodal imaging-guided synergistic photo-immunotherapy. *Bioact. Mat.* 6 (2), 312–325. doi:10.1016/j.bioactmat.2020.08.005

Finkel, T. (2011). Signal transduction by reactive oxygen species. *J. Cell Biol.* 194 (1), 7–15. doi:10.1083/jcb.201102095

Hall, E. D., Vaishnav, R. A., and Mustafa, A. G. (2010). Antioxidant therapies for traumatic brain injury. *Neurotherapeutics* 7 (1), 51–61. doi:10.1016/j.nurt.2009.10.021

He, H., Han, H., Shi, H., Tian, Y., Sun, F., Song, Y., et al. (2016). Construction of thermophilic lipase-embedded metal–organic frameworks via biomimetic mineralization: A biocatalyst for ester hydrolysis and kinetic resolution. *ACS Appl. Mat. Interfaces* 8 (37), 24517–24524. doi:10.1021/acsami.6b05538

- He, L., Huang, G., Liu, H., Sang, C., Liu, X., and Chen, T. (2020). Highly bioactive zeolitic imidazolate framework-8-capped nanotherapeutics for efficient reversal of reperfusion-induced injury in ischemic stroke. *Sci. Adv.* 6 (12), eaay9751. doi:10.1126/sciadv.aay9751
- Hoseinpour, V., and Shariatnia, Z. (2021). Applications of zeolitic imidazolate framework-8 (ZIF-8) in bone tissue engineering: A review. *Tissue Cell* 72, 101588. doi:10.1016/j.tice.2021.101588
- Hu, P., and Tirelli, N. (2012). Scavenging ROS: Superoxide dismutase/catalase mimetics by the use of an oxidation-sensitive nanocarrier/enzyme conjugate. *Bioconjug. Chem.* 23 (3), 438–449. doi:10.1021/bc200449k
- Jiang, W., Wang, X., Chen, J., Liu, Y., Han, H., Ding, Y., et al. (2017). Deuterohemin-peptide enzyme mimic-embedded metal-organic frameworks through biomimetic mineralization with efficient ATRP catalytic activity. *ACS Appl. Mat. Interfaces* 9 (32), 26948–26957. doi:10.1021/acsami.7b09218
- Li, Q., Chen, Y., Bai, S., Shao, X., Jiang, L., and Li, Q. (2020). Immobilized lipase in bio-based metal-organic frameworks constructed by biomimetic mineralization: A sustainable biocatalyst for biodiesel synthesis. *Colloids Surfaces B Biointerfaces* 188, 110812. doi:10.1016/j.colsurfb.2020.110812
- Li, Q., Liu, Y., Dai, X., Jiang, W., and Zhao, H. (2021). Nanozymes regulate redox homeostasis in ROS-related inflammation. *Front. Chem.* 9, 740607. doi:10.3389/fchem.2021.740607
- Li, Q., Liu, Y., Zhang, Y., and Jiang, W. (2022). Immunogenicity-boosted cancer immunotherapy based on nanoscale metal-organic frameworks. *J. Control. Release* 347, 183–198. doi:10.1016/j.jconrel.2022.05.003
- Li, Q., Shao, X., Dai, X., Guo, Q., Yuan, B., Liu, Y., et al. (2022). Recent trends in the development of hydrogel therapeutics for the treatment of central nervous system disorders. *NPG Asia Mat.* 14, 14. doi:10.1038/s41427-022-00362-y
- Lian, X., Chen, Y.-P., Liu, T.-F., and Zhou, H.-C. (2016). Coupling two enzymes into a tandem nanoreactor utilizing a hierarchically structured MOF. *Chem. Sci.* 7 (12), 6969–6973. doi:10.1039/c6sc01438k
- Lian, X., Fang, Y., Joseph, E., Wang, Q., Li, J., Banerjee, S., et al. (2017). Enzyme--MOF (Metal--Organic framework) composites. *Chem. Soc. Rev.* 46 (11), 3386–3401. doi:10.1039/c7cs00058h
- Liang, K., Coghlan, C. J., Bell, S. G., Doonan, C., and Falcaro, P. (2016). Enzyme encapsulation in zeolitic imidazolate frameworks: A comparison between controlled Co-precipitation and biomimetic mineralisation. *Chem. Commun.* 52 (3), 473–476. doi:10.1039/c5cc07577g
- Liang, K., Ricco, R., Doherty, C. M., Styles, M. J., Bell, S., Kirby, N., et al. (2015). Biomimetic mineralization of metal-organic frameworks as protective coatings for biomacromolecules. *Nat. Commun.* 6, 7240. doi:10.1038/ncomms8240
- Liu, Y., Hong, H., Xue, J., Luo, J., Liu, Q., Chen, X., et al. (2021). Near-infrared radiation-assisted drug delivery nanoplatfrom to realize blood-brain barrier crossing and protection for parkinsonian therapy. *ACS Appl. Mat. Interfaces* 13 (31), 37746–37760. doi:10.1021/acsami.1c12675
- Liu, Y., Li, Q., Bai, Q., and Jiang, W. (2021). Advances of smart nano-drug delivery systems in osteosarcoma treatment. *J. Mat. Chem. B* 9, 5439–5450. doi:10.1039/d1tb00566a
- Mehta, J., Bhardwaj, N., Bhardwaj, S. K., Kim, K.-H., and Deep, A. (2016). Recent advances in enzyme immobilization techniques: Metal-organic frameworks as novel substrates. *Coord. Chem. Rev.* 322, 30–40. doi:10.1016/j.ccr.2016.05.007
- Montanari, R. M., Barbosa, L. C. A., Demuner, A. J., Silva, C. J., Andrade, N. J., Ismail, F., et al. (2012). Exposure to anacardiaceae volatile oils and their constituents induces lipid peroxidation within food-borne bacteria cells. *Molecules* 17 (8), 9728–9740. doi:10.3390/molecules17089728
- Orellana-Tavra, C., Baxter, E. F., Tian, T., Bennett, T. D., Slater, N. K. H., Cheetham, A. K., et al. (2015). Amorphous metal--organic frameworks for drug delivery. *Chem. Commun.* 51 (73), 13878–13881. doi:10.1039/c5cc05237h
- Popa-Wagner, A., Mitran, S., Sivanesan, S., Chang, E., and Buga, A.-M. (2013). ROS and brain diseases: The good, the bad, and the ugly. *Oxid. Med. Cell. Longev.* 2013, 1–14. doi:10.1155/2013/963520
- Sena, L. A., and Chandel, N. S. (2012). Physiological roles of mitochondrial reactive oxygen species. *Mol. Cell* 48 (2), 158–167. doi:10.1016/j.molcel.2012.09.025
- Seshadri, G., Sy, J. C., Brown, M., Dikalov, S., Yang, S. C., Murthy, N., et al. (2010). The delivery of superoxide dismutase encapsulated in polyketal microparticles to rat myocardium and protection from myocardial ischemia-reperfusion injury. *Biomaterials* 31 (6), 1372–1379. doi:10.1016/j.biomaterials.2009.10.045
- Tabrez, S., R Jabir, N., Shakil, S., H Greig, N., Alam, Q., M Abuzenadah, A., et al. (2012). A synopsis on the role of tyrosine hydroxylase in Parkinson's disease. *CNS Neurol. Disord. Targets (Formerly Curr. Drug Targets-CNS Neurol. Disord.)* 11 (4), 395–409. doi:10.2174/187152712800792785
- Tong, J., Yi, X., Luxenhofer, R., Banks, W. A., Jordan, R., Zimmerman, M. C., et al. (2012). Conjugates of superoxide dismutase 1 with amphiphilic poly (2-oxazoline) block copolymers for enhanced brain delivery: Synthesis, characterization and evaluation *in vitro* and *in vivo*. *Mol. Pharm.* 10 (1), 360–377. doi:10.1021/mp300496x
- Van Raamsdonk, J. M., and Hekimi, S. (2012). Superoxide dismutase is dispensable for normal animal lifespan. *Proc. Natl. Acad. Sci. U. S. A.* 109 (15), 5785–5790. doi:10.1073/pnas.1116158109
- Wang, G., Liu, X., Guo, Q., and Namura, S. (2010). Chronic treatment with fibrates elevates superoxide dismutase in adult mouse brain microvessels. *Brain Res.* 1359, 247–255. doi:10.1016/j.brainres.2010.08.075
- Wu, M.-X., and Yang, Y.-W. (2017). Metal--Organic framework (MOF)-Based drug/cargo delivery and cancer therapy. *Adv. Mat.* 29 (23), 1606134. doi:10.1002/adma.201606134
- Xie, H., Hu, L., and Li, G. S. H.-S. Y5Y. (2010). SH-SY5Y human neuroblastoma cell line: *In vitro* cell model of dopaminergic neurons in Parkinson's disease. *Chin. Med. J.* 123 (8), 1086–1092.
- Yan, M. H., Wang, X., and Zhu, X. (2013). Mitochondrial defects and oxidative stress in alzheimer disease and Parkinson disease. *Free Radic. Biol. Med.* 62, 90–101. doi:10.1016/j.freeradbiomed.2012.11.014
- Yang, Y., Zhu, D., Liu, Y., Jiang, B., Jiang, W., Yan, X., et al. (2020). Platinum-carbon-integrated nanozymes for enhanced tumor photodynamic and photothermal therapy. *Nanoscale* 12, 13548–13557. doi:10.1039/d0nr02800b
- Zhang, Y., Li, Q., Han, C., Geng, F., Zhang, S., Qu, Y., et al. (2022). Superoxide dismutase@zeolite imidazolate framework-8 attenuates noise-induced hearing loss in rats. *Front. Pharmacol.* 13, 885113. doi:10.3389/fphar.2022.885113
- Zhu, D., Ling, R., Chen, H., Lyu, M., Qian, H., Wu, K., et al. (2022). Biomimetic copper single-atom nanozyme system for self-enhanced nanocatalytic tumor therapy. *Nano Res.* 15 (8), 7320–7328. doi:10.1007/s12274-022-4359-6
- Zhu, Y., Zhang, J., and Zeng, Y. (2012). Overview of tyrosine hydroxylase in Parkinson's disease. *CNS Neurol. Disord. Targets (Formerly Curr. Drug Targets-CNS Neurol. Disord.)* 11 (4), 350–358. doi:10.2174/187152712800792901